Interference Heads-Up
Receiver Techniques for Detecting and Characterizing RFI

Phillip W. Ward

AS WE ALL KNOW, GPS SIGNALS ARE WEAK. At a receiver's antenna, in the open air, their strength is about −160 dBW or 1 × 10⁻¹⁶ watts. Compare this to a cell-phone signal, which might be −60 dBW or 1 × 10⁻⁶ watts — 10 billion times stronger! While code correlation in the receiver lifts the GPS signals above the background noise floor, the signals are still relatively fragile, and building walls and other obstructions can significantly attenuate the received signal power so that they cannot be tracked by a conventional receiver.

It is the ratio of the signal power to the noise power per unit band-width that determines the trackability of the signal. Accordingly, if the receiver's noise floor should increase sufficiently, even in an outdoor environment, the signals may also become untrackable. This can happen when the receiver is subjected to intentional or unintentional radio-frequency interference (RFI) by a transmitter operating on or near GPS frequencies. If the interference is strong enough, it can jam the receiver. Although intentional jamming is typically of concern only to military GPS users, unintentional jamming can occur anywhere and any-time and can affect large numbers of users within the range of the jamming transmitter. The jamming incident in San Diego harbor in January 2007, for exam-ple, affected all GPS users within a range of about 15 kilometers including a medical services paging network.

Such jamming renders a GPS receiver inoperable. But how do users know that their receivers are being jammed and not suffering some other type of malfunction? Clearly it would be advantageous for users to receive a heads-up when jamming signals are present and, if possible, for the receiver to take corrective action automatically.

In this month's column, we look at some simple techniques, which can be easily incorporated into the design of a GNSS receiver, to detect, characterize, and actually mitigate RFI. Such receiver enhancements will benefit civilian and military users alike.

INNOVATION INSIGHTS
with Richard Langley

Unintentional jamming

can occur anywhere

and anytime.

With the growing proliferation of a large variety of transmit-ters around the world, there should be little question that the noise floor for GNSS receivers will continue to increase along with the threat of dis-abling in-band radio-frequency interfer-ence (RFI). RFI poses a serious threat to the reliable operation of GNSS receivers when the received RFI power level is high enough to render the GNSS receiver in-operable. RFI that is at or beyond the tol-erable jamming capability of the GNSS receiver (which is related to the receiver's background thermal noise level) causes no end of confusion to the user. There are usually no visible external signs of anything being out of order, so the user initially assumes the receiver has experi-enced an internal failure.

Without the sophistication of built-in RFI situational awareness in the GNSS receiver design, the determina-tion of the presence and seriousness of in-band RFI problems is an extremely inefficient and frustrating process. A simple jamming-to-noise-power (J/N) monitor can be a low-cost built-in fea-ture of the GNSS receiver if a J/N me-ter design is preplanned in the original GNSS receiver front-end component design, layout, and implementation. A retrofit to an existing design is usually impractical. An additional justification for including a J/N meter in the initial GNSS receiver design is the signifi-cant performance advantages obtained through RFI situational adaptation especially during initial search. Every GNSS receiver user who anticipates or has ever experienced an operational failure due to in-band RFI will greatly value this feature. Certainly, all safety-of-life GNSS applications and the mili-tary should require it.
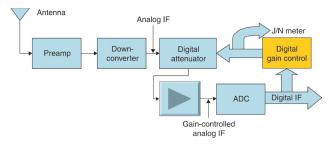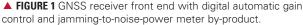
J/N Meter Design

FIGURE 1 is a high-level functional block diagram of a GNSS receiver RF front end that contains a J/N meter that is obtained as a byproduct of the digital gain control part of the digital automatic gain control (AGC) design. **FIGURE 2** is an expanded functional block diagram of the digital gain control function shown in Figure 1. The J/N meter design shown in Figure 1 is implemented in the last intermediate frequency (IF) stage of the GNSS receiver RF front-end architecture — that is, prior to signal detection by the multiple digital receiver channels (not shown in the figure). At the last receiver IF stage, the GNSS spread spectrum received signal power (S_{IF}) from each satellite in view is well below the thermal noise power (N_{IF}). This assumes the receiver is located on or near the surface of the Earth and the antenna gain is in the region of near unity gain with respect to an ideal isotropic circularly polarized antenna (0 dBic).
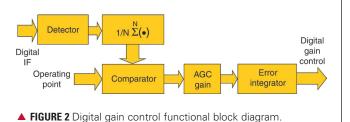
For a typical unjammed wideband (WB) C/A-code receiver example, S_{IF} is typically 30 dB below N_{IF} at the last IF stage, so $(S/N)_{IF} = S_{IF} - N_{IF} = -30$ dB; that is, the C/A-code signal power is a thousand times lower in power than the thermal noise power just before the signal detection process takes place in the digital receiver channels. A key point to remember is that all GNSS spread spectrum signals are designed so they can be readily acquired and tracked even though $(S/N)_{IF}$ is considerably negative. When in-band RFI jamming power (J_{IF}) is present at IF, the effective noise level is increased so that the receiver may be unable to acquire and track the GNSS signals in view. Since the undetected signal is always below the noise level (whether or not J_{IF} is present), it is impossible to obtain a measure of the composite signal-to-noise power ratio at IF. This is usually designated as the signal-to-noise plus interference power ratio at IF $(SNIR)_{IF}$.

If the GNSS receiver is tracking the space vehicle (SV) signals, then at baseband the SNIR can be accurately measured by the receiver baseband process. It is common practice to measure the carrier-to-noise power ratio in a 1 Hz noise bandwidth $(C/N_0 = S/N_0)$ at baseband as a signal quality indicator for each SV being tracked. In this case, the SV signals have been acquired (despread) and the processing gain obtained by despreading results in a positive SNIR, thereby permitting the measure of C/N_0 at baseband. However, if the RFI is so severe that the baseband SNIR approaches or is below 0 dB (unity linear ratio), then the SV signals cannot be acquired or tracked by the GNSS receiver. Since it is impossible to measure the SNIR at baseband if the RFI power level prevents signal detection, this method does not provide a total RFI situational awareness technique. In other words, the traditional measure of C/N_0 at baseband is necessary, but not sufficient for total RFI situational awareness.

However, total RFI situational awareness is practical because the presence of RFI can be accurately measured at the RF front-end output, namely at IF. It cannot be measured with respect to S_{IF} but it can be measured with respect to

▲ **FIGURE 1** GNSS receiver front end with digital automatic gain control and jamming-to-noise-power meter by-product.

▲ **FIGURE 2** Digital gain control functional block diagram.

the unjammed thermal noise power level at IF ($N_{IFtherm}$) that has been measured and stored in memory during the GNSS receiver built-in test operation. Using the stored value of the unjammed thermal noise level, $N_{IFtherm}$, as the reference level and the current reading as the jamming level, J_{IF}, the J/N meter measurement is obtained from $J_{IF} - N_{IFtherm}$ in units of dB. S_{IF} is so far below the noise level at IF that it can be considered negligible (zero) for purposes of this measurement and the AGC amplifier is designed so that the gain is linear in dB. Note that in the absence of RFI above the thermal noise level, the J_{IF} reading is equal to $N_{IFtherm}$ so the J/N meter reading is 0 dB. The J/N meter cannot measure negative J/N. Also note that, for every increase of J_{IF} in dB thereafter, this corresponds to the increase in RFI level in dB with respect to the calibrated unjammed thermal noise level, $N_{IFtherm}$.

The J/N meter provides an excellent measure of the RFI threat to the GNSS receiver because $N_{IFtherm}$ is always an acceptable amount of noise for reliable signal acquisition, with one possible exception. Continuous wave (CW) noise power just below the thermal noise level can be problematic to the acquisition of the GPS L1 C/A-code signals.

RF Front End

Referring to the Figure 1 functional block diagram of the GNSS receiver RF front end with AGC digital gain control and J/N meter, the analog components begin with a right-hand circularly polarized L-band antenna with nearly hemispherical gain coverage. This is followed by an L-band preamplifier and downconverter and ends with an AGC amplifier at the IF stage. At this point, the L-band signal has been amplified by nearly 100 dB, signal-conditioned (filtered), and translated from L-band to the IF center frequency. The gain-controlled analog IF signal is converted to a digital IF signal by the sampling and quantization process of the analog-to-digital converter (ADC). Thereafter,

all GNSS receiver processes are digital. The thick signal flow lines in Figure 1 portray that these digital signal paths typically contain multiple bits. The digital gain control uses the ADC digital output to close the AGC loop. Each L-band GNSS signal requires separate down-conversion ending in a separate ADC with a digital IF output. Note that at this point all of the GNSS signals in view are still buried in noise.

The digital IF signals are provided to multiple digital receiver channels that are under the control of a receiver processor (both not shown in this block diagram). If multiple L-band down-conversions to the same IF have been performed, for example the GPS L1 and L2 signals, then each digital receiver selects the appropriate IF to search and track. Also not shown are the reference oscillator and frequency synthesizer, essential RF front-end analog components that support the down-conversion process and the synchronization of the digital signal processing functions to the real-time analog signals.

The digital gain control of Figure 1 is expanded in the functional block diagram of Figure 2. The digital IF signal from the ADC is fed to the detector, which rectifies the signal and passes it to an averaging function that sums N samples of the IF, then divides the result by N. This function sets the attack and recovery rates of the AGC. The output is fed to one side of a digital comparator. The AGC root-mean-square amplitude is set by the digital value of the operating point that is applied to the other side of the comparator. The error output of the comparator is scaled appropriately for the AGC attenuator by the AGC gain stage. The final stage of the digital gain control is the error integrator. The digital gain control output not only controls the AGC amplifier gain, it also provides the J/N meter reading.

For more design details, including the calibration and J/N measurement algorithms, refer to the references in Further Reading.

Estimating J/S from J/N

A conservative estimation of J/S at IF based on the observed J/N measurement at IF uses the specified minimum received signal power, S_{MIN}, in dBW. The computation requires *a priori* knowledge of the antenna noise temperature, T_{ant}, in kelvins (K), the receiver amplifier noise figure, N_f, in dB at 290 K, and the RF front-end bandwidth, B_{fe}, in Hz. The J/S estimate is computed using Equation (1) where the noise power is determined using the values and expressions in **TABLE 1**.

$$J/S = J/N + N - S_{MIN} \qquad (1)$$

As a computational example, assume that a C/A-code receiver is being analyzed so $S_{MIN} = -158.5$ dBW. The *a priori* parameter assumptions are: antenna noise temperature = 100 K; amplifier noise figure = 4.3 dB at 290 K; and $B_{fe} = 18 \times 10^6$ Hz (a high performance wideband C/A-code receiver). Working from the bottom up using the stepwise computation from Table 1 and Equation (1), we obtain the values

TABLE 1. Terms in the calculation of J/S

Symbol	Definition	Units	Expression/Value
N	thermal noise power in a B_{fe} bandwidth	dBW	$N_0 - 10 \log (1/B_{fe})$
N_0	thermal noise power in a 1 Hz bandwidth	dBW	$10 \log [k(T_{ant} + T_{amp})]$
k	Boltzmann constant	J/K	$1.380\ 6504 \times 10^{-23}$
T_{amp}	amplifier temperature	K	$290\ [10^{(N_f/10)} - 1]$

TABLE 2. J/S example

Parameter	Computation	Value
T_{amp}	$290\ (10^{0.43} - 1)$	490.5 K
N_0	$10 \log [1.380\ 6504 \times 10^{-23}\ (100 + 490.5)]$	-200.9 dBW
N	$-200.9 - 10 \log [1/(18 \times 10^6)]$	-128.3 dBW
J/S	$J/N - 128.3 + 158.5$	J/N + 30.2 dB

in **TABLE 2**. The J/S value is about 30 dB above the J/N value.

Adaptive Initial Search Using J/N Meter

The J/N meter provides a new opportunity to improve initial signal acquisition, especially if the noise is characterized before initial signal acquisition is attempted. The J/N meter combined with signal characterization permits the search process to be adapted to it using an optimized (increased) dwell time, T, during search and increased predetection integration time, T, after transition to tracking. Refer to the Further Reading background papers for an example of search optimization with variable T using the J/N meter situational awareness and the assumption that the RFI is band-limited white noise (BLWN).

The good news for future generations of GNSS receivers is that modernized GNSS signals offer "dataless" replica code choices that permit longer T than the current GPS L1 C/A and L1/L2 P(Y) signals. Because of the presence of 50 Hz data modulation, these signals limit $T \leq 10$ milliseconds during search and $T \leq 20$ milliseconds during track modes. After the data transition boundary is determined by a bit-synchronization process, a complicated process called "data wipeoff" can be employed to increase T during track modes for each SV if the current data-bit pattern has been provided by some external means or has been recently learned after 12.5 minutes of error-free data demodulation (the complete navigation message lasts 12.5 minutes). "Data wipeoff" is of no use during initial search when the data transition boundaries for the SVs are unknown.

Removing CW and NB RFI

There is a well-known process called *spectral excision* that can suppress CW and narrow-band (NB) noise to the current noise floor. Spectral excision is usually performed at IF. One approach uses a digital signal processor (DSP) to perform a discrete Fourier transform (DFT) of the digitized IF signal over a statistically significant time interval. The spectral envelope

over the resulting discrete frequency interval is inspected and the noise floor determined. Any CW or other NB spectral amplitude outliers are clipped off at this noise floor in the discrete frequency domain. This throughput-intensive process ends with the inverse-DFT that sends the spectrally excised discrete time-domain digital IF signals on to all of the digital receiver channels. The process is then repeated contiguously for each DFT time interval thereafter.

Alternatively, a transversal digital filter can be implemented at IF, which accomplishes NB spectral excision. The transversal filter design is used if an application specific integrated circuit (ASIC) hardware implementation is preferred over a DSP.
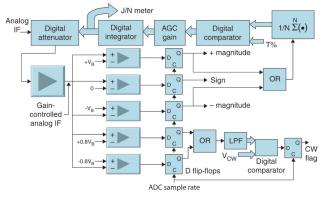
In both cases, the ADC must quantize each IF sample with 10 to 12 bits or more precision to provide the amplitude resolution necessary to support a meaningful spectral excision process. Also, the IF digital sample rates for these two processes are of the order of 5 mega-samples per second (Msps) for a NB C/A-code receiver ($B_{fe} = 1.8$ MHz), 50 Msps for a P(Y)-code or WB C/A-code receiver ($B_{fe} = 18$ MHz), and 70 Msps for an M-code receiver ($B_{fe} = 24$ MHz). Needless to say, spectral excision is a highly complex and expensive GNSS receiver design feature. Spectral excision techniques have little or no effect on WB RFI.

Antenna null steering (forming gain nulls toward the jammer(s)) and/or beam steering (forming gain peaks toward the SVs) are the only means for minimizing WB RFI, except for pulsed RFI (described later). Assuming a fixed-reception-pattern antenna is used and external aiding is not used, the only simple means of enhancing the robustness of a GNSS receiver against WB RFI, except in the case of pulsed RFI (again, described later), is the optimization of the search and tracking designs. Hence, the quest for simple means of mitigating and characterizing RFI is confined to constant envelope NB RFI, especially CW RFI, but all RFI is measured by the simple J/N meter.

RFI Characterization

RFI is usually characterized as being WB or NB. NB includes CW RFI, and WB includes matched spectrum, BLWN, and pulsed RFI. Pulsed RFI is addressed last in this article. Null-to-null BLWN has about half of the adverse effect on a GNSS receiver as NB RFI for the same amount of in-band power. Matched spectrum is about halfway between the two. So, in order to determine how lethal is the RFI power level as measured by the J/N meter, the RFI should also be characterized.

RFI characterization is derived from the statistical distribution of the IF noise amplitudes. A sophisticated computation of the probability density at IF involves sorting a statistically significant number of digital amplitude samples additively into discrete amplitude bins. The number of bins depends on the desired discrete amplitude resolution. At the end of the collection interval, the bins are normalized by the total num-

▲ **FIGURE 3** Simple automatic gain control with non-uniform analog-to-digital conversion, jamming-to-noise-power meter, and continuous wave detector.

ber of samples taken. The normalized amplitude distribution characteristic is then examined. The composite IF noise is then characterized based on recognizing the amplitude distribution pattern. The data-gathering process is computationally intensive and the recognition process is complicated.
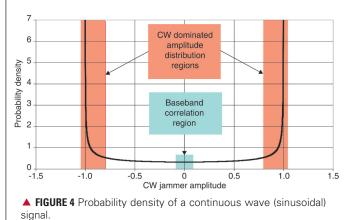
Simple CW RFI Effect Minimization. Fortunately, simple design techniques can minimize and characterize constant envelope NB RFI, hereafter discussed in the context of CW RFI. **FIGURE 3** illustrates a design example of a non-uniform ADC that not only provides a J/N meter to measure the RFI level, but also detects the presence of CW RFI at IF and minimizes the effect. The functional similarity between the upper part of Figure 3 and Figures 1 and 2 should be readily apparent. This synergistic combination of simple designs provides significant RFI-effect minimization at relatively low cost.

Referring to Figure 3, the non-uniform three-level (1.5 bit) flash ADC is designed to provide substantial processing gain in the presence of CW interference plus thermal noise. It significantly outperforms an infinite-bit ADC in the presence of CW RFI. As a result of CW RFI, the statistics of the zero crossings of the signal are no longer determined by a combination of thermal noise and the GPS signals that are buried in this random noise, but become dominated by the statistics of the CW signal. The probability density of a CW (sinusoidal) signal is given by:

$$P(x) = \frac{1}{\pi \sqrt{1 - x^2}} \qquad (2)$$

where x is a random variable in the range of ± 1, but can be treated as the normalized peak-to-peak amplitude of the sinusoid. Equation 2 is plotted in **FIGURE 4**. Observe in this plot that the CW signal spends most of its time near the peak amplitudes rather than in the vicinity of the zero crossing. Keep in mind that thermal noise has a Gaussian probability density so that, statistically, the GNSS signals plus thermal noise are predominantly in the vicinity of the zero crossing. Thus, even though the thermal noise power can be three orders of magnitude above the GNSS signal levels at IF, the statistics of the signal zero crossings

▲ **FIGURE 4** Probability density of a continuous wave (sinusoidal) signal.

are such that the correlation processes succeed. However, strong CW signals in combination with the weak GNSS signals plus thermal noise causes the composite signal to spend very little time near the zero crossing, so the correlation processes are adversely affected. The adverse consequence is that correlation is possible only a very low percentage of the time. This effect is illustrated in Figure 4.

Referring to the upper part of Figure 3, the non-uniform ADC minimizes this problem by adjusting the peaks of the composite CW signal with respect to the non-uniform bias levels of the plus and minus magnitude-bit comparators. These bias levels are the reference voltages $+V_B$ and $-V_B$, respectively. The T% (of V_B) control in the AGC feedback loop adjusts the CW signal amplitude (when CW is present) so that the CW peak is T% above $+V_B$ and below $-V_B$. As a result, for a T% bound in the CW regions around $+V_B$ and $-V_B$, the plus and minus magnitude-bit comparators behave in a manner during the CW peaks similar to the sign-bit comparator during zero crossings in the presence of only thermal noise. As part of the AGC feedback control, the weighting factor, N, adjusts the statistical averaging time to properly follow fluctuations in the noise level at IF.
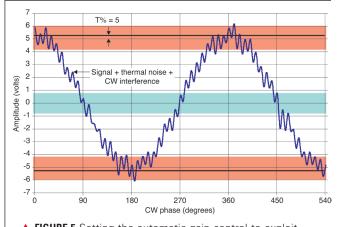
FIGURE 5 depicts the thermal noise added to (riding on top

▲ **FIGURE 5** Setting the automatic gain control to exploit constant envelope interference statistics using non-uniform analog-to-digital-conversion thresholds.
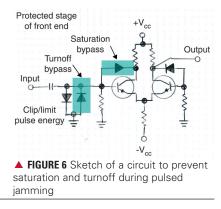
of) a composite CW signal along with typical complementary threshold settings of T% = 5. The GNSS signals are so far below the thermal noise that they cannot be observed in Figure 5, but the thermal noise provides the desired statistical distribution around the $+V_B$ and $-V_B$ regions. Consider also that there is only a small fraction of a chip of any GNSS signal present during several cycles of any in-band CW signal. Observe that Figure 5 illustrates how the T% threshold adjusts the signal statistics such that a similar effect is taking place at the plus magnitude-bit ($+V_B$ reference) and minus magnitude-bit ($-V_B$ reference) comparators as would occur at the sign-bit comparator (0 volt reference) with only thermal noise present. In this manner, the non-uniform ADC provides correlation in the presence of CW interference.

The values of T% and N can be constants or adaptive variables depending on the level of sophistication desired. If variable, then the J/N meter (described earlier) and the CW signal detector (CW flag) in the lower portion of Figure 3 are used to make the adjustments dynamically. The range of T% is adjusted typically between 5 and 15 and N typically between 4 and 16, depending on CW being present and the level of CW interference as indicated by these built-in monitors. As a guideline, for the GPS C/A-code the best CW performance at the highest J/N is achieved when T% is 5 and N is 16. There is less signal degradation at the lowest J/N conditions if T% is 15 and N is 4. The specific design requires tuning.

At this point, it should be obvious to the reader that the 1.5-bit non-uniform ADC would not be compatible with DFT or transversal filter frequency excision techniques.

Simple CW Detector Design. A simple CW detector design is depicted in the lower part of Figure 3. The two lower analog comparators with reference voltages $+0.8\,V_B$ and $-0.8\,V_B$, along with the D-type flip-flops, provide a flash ADC measure of the IF amplitude density in the region dominated by CW RFI. Note that multiple sources of CW RFI of various powers combine into one composite CW characterization. Following the flash ADC are the OR gate, low-pass filter, digital comparator, and D flip-flop that combine to produce the CW flag. The digital comparator threshold voltage, V_{CW}, is chosen to determine when the statistics are such that CW is the dominating IF signal. Any time this threshold is exceeded, the CW flag is set to "1" (true); otherwise it is set to "0" (false). This design operates in concert with the AGC being controlled to keep the AGC amplifier gain adjusted so that any CW-dominated signal will have its peak at T% above and below $+V_B$ and $-V_B$, respectively. The J/N meter provides RFI situational awareness of the RFI level and the CW flag provides a warning when the RFI is dominated by CW. In fact, the warning occurs when any constant envelope NB RFI is present. These are the two most important RFI situational awareness attributes to monitor. By inference, if the J/N meter indicates that RFI is present and the CW flag is "false," the most likely characterization is WB RFI.

Mitigation Techniques. There are few simple wideband

▲ **FIGURE 6** Sketch of a circuit to prevent saturation and turnoff during pulsed jamming

RFI mitigation techniques, but low-duty-cycle pulsed RFI, such as from radar transmissions, can be circumvented by two relatively simple GNSS RF front-end design techniques. First, the AGC attack and recovery times should be designed to be as fast as possible. Specifically, the AGC attack and recovery time intervals should be an order of magnitude smaller than the shortest practical search dwell time or track predetection integration time. Since the minimum is typically 500 microseconds for a meaningful correlation interval, then the attack and recovery times should be as close to 50 microseconds as possible — consistent with the AGC closed loop feedback stability. In any case, the AGC time constant should be much less than 1 millisecond. Second, all analog gain stages of the RF front end should be prevented from being saturated or completely turned off by high-energy pulsed RFI sources. The reason for this is that if the AGC and the RF front end follow the signal blanking effect of the pulsed RFI energy by rapid gain compression and expansion responses, the relatively short period of time that signal correlation is lost will have only a small order effect on the GNSS receiver operation. For example, if the pulsed RFI duration is less than a few microseconds and the duty cycle of the pulsed energy is 50%, a well-designed GNSS receiver is blanked for about 50% of the time. This reduces the unjammed C/N_0 by about 3 dB. Assuming an unjammed C/N_0 of 40 dB-Hz, then the receiver should operate through the pulsed RFI with a reduced C/N_0 of about 37 dB-Hz.

FIGURE 6 depicts the use of back-to-back PIN diodes to clip the high-energy pulses at the input of each RF front-end gain stage (a PIN diode is a fast-acting diode with an intrinsic or undoped semiconductor sandwiched between the usual p-type and n-type semiconductors). One of these diodes also becomes forward biased before the base-emitter voltage level reaches the point where the transistor turns completely off. It also shows the use of reversed biased base-to-collector diodes added to each transistor to shunt excess transistor base current into the transistor collector-emitter path to pre-

vent saturation. Thus, the non-uniform actions of a few diodes prevent RF front-end saturation or cutoff during gain compression due to high-energy pulsed RFI bursts. The diodes also prevent damage to the RF front end by excessive energy bursts. Without the non-uniform actions of the diodes, the long recovery times after saturation or turnoff result in continuous gain compression (non-operation).

Conclusion

In this article, we have looked at RFI mitigation techniques and receiver design trade-offs, including a simple but highly effective mitigation technique for CW and other constant envelope NB RFI. The overview included a specific GNSS front-end design that includes a J/N meter. The mitigation scheme is implemented using a simple non-uniform ADC design in combination with a novel AGC design.

There is a need to characterize the RFI when the J/N meter determines it is present because different types of RFI have different effects on the GNSS receiver. Prior to search and acquisition, it is especially important to determine the presence of CW and other types of constant envelope NB RFI because these are the most lethal, albeit the easiest to mitigate.

Simple mitigation techniques for pulsed RFI, a typical source of WB RFI for commercial GNSS receivers, have also been described. These techniques effectively neutralize most pulsed RFI and they offer protection to the RF front end for any high-energy RFI.

Acknowledgments

PHILLIP WARD is president of Navward GPS Consulting, which he founded in October 1991 in Dallas, Texas. Prior to becoming a consultant, he was senior member of the Technical Staff in the Defense Systems & Electronics Group of Texas Instruments Incorporated. He has been involved in the field of navigation since 1958 and with GPS receiver design as a systems engineer since 1976. He received his B.S.E.E. degree from the University of Texas at El Paso and his M.S.E.E. degree from Southern Methodist University in Dallas. He is a registered professional engineer in the state of Texas.

MORE ONLINE
Further Reading

FURTHER READING

• Radio Frequency Interference in GNSS Receivers

"Simple Techniques for RFI Situational Awareness and Characterization in GNSS Receivers" by P. Ward in *Proceedings of The Institute of Navigation 2008 National Technical Meeting*, San Diego, California, January 28-30, 2008, pp. 154-163.

"What's Going On? RFI Situational Awareness in GNSS Receivers" by P. Ward in *Inside GNSS*, Vol. 2, No. 6, September/October 2007, pp. 34-42.

"Interference, Multipath, and Scintillation" by P. Ward, J. Betz, and C. Hegarty in *Understanding GPS: Principles and Applications*, Second Edition, E. Kaplan and C. Hegarty, Eds., Artech House, Inc., 2006.

• GNSS Signal Acquisition and Tracking

"Satellite Signal Acquisition, Tracking, and Data Demodulation" by P. Ward, J. Betz, and C. Hegarty in *Understanding GPS: Principles and Applications*, Second Edition, E. Kaplan and C. Hegarty, Eds., Artech House, Inc., 2006.

• CW Interference

"Adaptive A/D Converter to Suppress CW Interference in DSPN Spread-Spectrum Communications" by F. Amoroso in *IEEE Transactions on Communications*, Vol. Com-31, No. 10, October 1983, pp. 1117-1123.

• Previous GPS World Articles on Radio Frequency Interference

"Jamming Protection of GPS Receivers – Part II: Antenna Enhancements" by S. Rounds in *GPS World*, Vol. 15, No. 2, February 2004, pp. 38-45.

"Jamming Protection of GPS Receivers – Part I: Receiver Enhancements" by S. Rounds in *GPS World*, Vol. 15, No. 1, January 2004, pp. 54-59.

"Jamming GPS: Susceptibility of Some Civil GPS Receivers" by B. Forssell and T.B. Olsen in *GPS World*, Vol. 14, No.1, January 2003, pp. 54-58.

"Radiofrequency Interference and GPS: A Growing Concern" by F. Butsch in *GPS World*, Vol. 13, No. 10, October 2002, pp. 40-50.

"Interference: Sources and Symptoms" by R. Johannessen in *GPS World*, Vol. 8, No. 11, November 1997, pp. 44-48.